J|A|C|S
COMMUNICATIONS

Published on Web 09/13/2006

Porous Carbon Powders Prepared by Ultrasonic Spray Pyrolysis

Sara E. Skrabalak and Kenneth S. Suslick*

School of Chemical Sciences, University of Illinois at Urbana−Champaign, 601 South Goodwin Avenue, Urbana, Illinois 61801

Received July 10, 2006; E-mail: ksuslick@uiuc.edu

Porous carbon materials are of interest for their potential use in electrochemical, catalytic, adsorbent, and gas-storage applications.[1] Until recently, most porous carbons were prepared by carbonization of raw natural materials[2] (e.g., wood, coal, petroleum pitches, coconut shell); as prepared, such carbons are either microporous (pore size <2 nm) or low surface area solids with broad pore-size distributions. Meso- (pore size 2−20 nm) and macroporous (>20 nm) carbons have gained recent prominence for applications involving large molecules (e.g., separations) and high diffusion rates (e.g., electrodes for double-layer capacitors, catalyst supports).[3] The synthesis of such materials, however, is less straightforward. Originally prepared by carbonization of either block copolymers with thermally unstable porogens or organic aerogels based on resorcinol−formaldehyde resins,[4] such materials are often unstable and volumetric shrinkage up to 70% has been reported.[4b] Recent research efforts emphasize the use of templates and their subsequent removal to produce meso- and macroporous carbons with controlled and, in some cases, periodic pores.[3] With this approach, a carbon precursor/inorganic template composite is first formed, followed by carbonization, then chemical leaching of the template material. Such methodology is tedious, requiring multiple synthetic steps, caustic chemical treatments, and long curing times; scale-up has also proven difficult[5] and is not cost-effective due to the destruction of (relatively) expensive templates.

Here, we use ultrasonic spray pyrolysis (USP)[6] as a continuous, one-step process for the generation of meso- and macroporous carbon powders. Our approach was to start with organic salts with easily dissociated leaving groups (e.g., CO_2, H_2O, HCl, SO_3) of an appropriate stoichiometry that would provide an inorganic salt and remnant carbon to form a highly cross-linked carbon network. Unlike most prior methodologies (with a few exceptions[7]), a *temporary template* (an inorganic salt) is generated in situ, which is then dissolved during aqueous workup.

The porous carbons are prepared by ultrasonically nebulizing aqueous solutions of alkali metal chloroacetate (CA), dichloroacetate (DCA), or other organic salts into droplets using a household humidifier (Supporting Information Figure 1). An Ar flow carries the droplets into a furnace, where solvent evaporation and precursor decomposition occurs, producing a carbon/inorganic salt composite. The product is collected in water bubblers with the generated salt dissolving, leaving behind the porous carbon.

Scanning electron micrographs (SEM) are shown in Figure 1 for USP products of 1.5 M aqueous solutions of lithium, sodium, and potassium CA and DCA pyrolyzed at 700 °C. A range of morphologies are observed, including hollow core−shell spheres (Figure 1a) and meso- (Figure 1d) and macroporous carbon networks (Figure 1b,c,e,f). Energy-dispersive X-ray (EDX) analysis and bulk elemental analysis confirm the formation of a predominantly carbon material, while further characterization indicates the formation of polyaromatic hydrocarbons.[8]

We have created a rational design criterion to our choice of precursors. If we assume that volatile, highly stable leaving groups

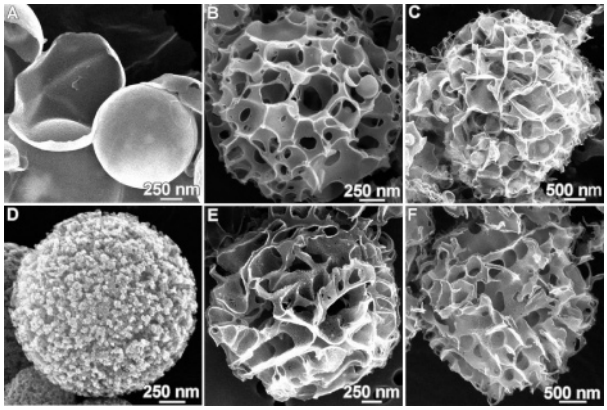

Figure 1. SEM images of USP porous carbons. Reaction conditions: 1.5 M solutions, 700 °C, Ar at 1.0 slpm. Product from (A) lithium chloroacetate, LiCA, (B) sodium chloroacetate, NaCA, (C) potassium chloroacetate, KCA, (D) lithium dichloroacetate, LiDCA, (E) sodium dichloroacetate, NaDCA, and (F) potassium dichloroacetate, KDCA.

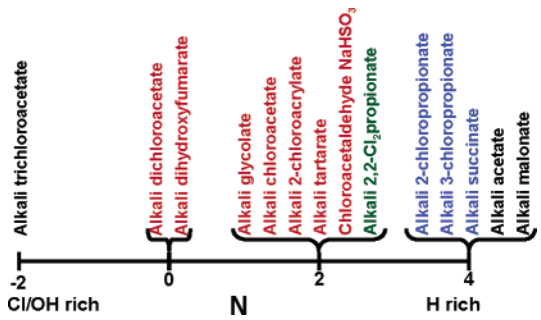

Figure 2. Preparation of porous carbon as a function of precursor stoichiometry. In red, precursors that generate spheres or networks through USP. In black, precursors that do not produce any product. In blue, precursors that produce ill-defined solids. In green, a precursor that produces mixed results. The precursors are clustered by the number *N*, defined by eq 1, which represents the excess (or deficit if negative) of hydrogen in the precursor necessary for ideal decomposition.

dissociate rapidly from heated droplets, then let us rearrange a general chemical formula to explicitly show the expected leaving groups, as in eq 1, where M = alkali metal ion and X = halide or hydroxyl.

$$M_mX_mC_n(CO_2 \text{ or } SO_3)_aH_bX_c \qquad (1)$$

For example, let us represent NaDCA (i.e., Cl_2HCCO_2Na) as NaCl C (CO_2) (HCl); upon thermal decomposition and loss of HCl and CO_2, one expects NaCl and a remnant carbon atom. For the ideal precursor, $b = c$; that is, after pyrolysis, the only remnant is carbon. If we now define $N = b - c$, then N represents the excess (or deficit if negative) of hydrogen in the precursor necessary for ideal decomposition. A complete list of precursors examined versus N is provided in Figure 2. As expected, if $N \sim 0$, we get good formation of carbon networks or spheres; otherwise, ill-defined

10.1021/ja064899h CCC: $33.50

carbon products result due to insufficient cross-linking. Alkali acetates and malonates were run as controls (since they cannot decompose through the proposed mechanism) and as expected, they do not form carbon networks.

It is interesting that such varied morphologies are obtained from seemingly similar precursors (e.g., Li, Na, K haloacetates). During these syntheses, the respective alkali metal chloride salt is formed and acts as a pore template. SEMs (Supporting Information Figure 2) of solids collected without water show a nonporous solid whose pores are clogged with salt (confirmed by EDX and XRD); upon washing, the salt dissolves and the carbon network is revealed.

The formation of the respective alkali metal salt, however, does not explain the different morphologies, particularly when comparing products from Li salts to those of Na and K. One might imagine that the difference in melting points of the generated salts (LiCl, mp 605 °C; NaCl, mp 801 °C; KCl, mp 770 °C) would be important; however, increasing the furnace temperature above 900 °C does not affect the morphologies.

One might also imagine that the amount of carbon generated compared to MX could be important. From the Lang Equation,[9] the aerosol droplets in our experiments are estimated to have a volume of ~13 μm^3. From 1.5 M precursor solutions, ~0.40 μm^3 of LiCl is generated per droplet, compared to 0.50 and 0.70 μm^3 of NaCl and KCl, respectively. Significantly, the difference in volume occupied by LiCl and NaCl is essentially the same as that between NaCl and KCl. While dramatic differences in morphology are observed between the products generated from Li and Na salts, no such differences are observed for Na versus K. It thus appears that carbon concentration is not a primary factor in determining morphology.

Minimally, there are four relevant processes that need to be considered when heating a droplet of a halocarboxylate salt (other than water evaporation). The organic salt may melt; the organic salt may exothermically decompose releasing MX; the organic salt may undergo endothermic decarboxylation; and the inorganic salt MX may melt. It is the relative order and kinetics of these processes that lead to the differences in morphology.

For example, the following scenario can be envisioned for carbon sphere-shell (Figure 1a) formation from heated aqueous droplets of LiCA: (1) water evaporates, leaving a droplet of solid LiCA; (2) the LiCA then begins to melt; (3) as the droplet temperature increases, the exterior LiCA decomposes, creating LiCl and carbon material; however, the interior, now molten, has yet to decompose; (4) the interior melt acts as a template and further source for the growing carbon shell. In this instance, the DSC and TGA data (Supporting Information Figure 3A) suggest that close precursor melting and decomposition temperatures are essential for the formation of core−shell carbon spheres via USP.

In contrast, LiDCA (which forms mesoporous carbon, Figure 1d) melts long before decomposition (Supporting Information Figure 3B). LiCl formation is closely coupled with decarboxylation, creating reactive sites for carbon network growth throughout an entirely molten droplet. Consistent with this, the DSC curve shows a multitude of endo- and exothermic peaks above 200 °C.

The Na and K salts of CA and DCA display a third class of decomposition in which no melting occurs before MX formation (Supporting Information Figure 3C−F). In this case, the carbon network forms through solid-state reactions. This difference likely promotes macropore formation by limiting diffusion of precursor and remnant carbon in the solid droplet.

The USP technique also affects the morphology of the resulting material. Besides generating nonagglomerated, micron-sized particles, the pore structures obtained through USP are different than those obtained from thermal decomposition of the precursors (Supporting Information Figure 4) in which meso- and small macropores are not always formed. As the USP technique generates discrete aerosol droplets, MX crystal growth and consolidation is limited by both the concentration of the precursor solution and the residence time within the furnace; this allows for better dispersion of MX throughout the growing carbon network.

As produced, the carbon powders described here could be used as adsorbents and gas-storage materials because of their varied pore structures and range of surface areas (e.g., NaCA product 70 m^2/g; LiDCA product 710 m^2/g; others ~200 m^2/g). For electrochemical and catalytic applications, porous carbons must maintain their structure during both processing and use at moderate temperatures. Both NaCA and LiDCA products are mechanically robust to stirring, grinding, and mild compaction. They are also thermally stable to carbonization (900 °C, 5 h). The enhanced stability of these two powders is likely due to more extensive cross-linking during carbon network formation.

The carbon materials described here are prepared through a new, facile synthetic method. We have developed a nontemplating spray pyrolysis method in which rationally selected precursors thermally decompose into an inorganic salt and a highly cross-linked carbon network. The generated salts act as temporary templates during carbon network formation and are easily removed upon aqueous workup.

Acknowledgment. These studies were supported by the NSF (CHE0315494) with characterizations carried out in the Center for Microanalysis of Materials, UIUC, which is partially supported by the U.S. DOE under grant DEFG02-91-ER45439.

Supporting Information Available: Experimental details, description of apparatus, and additional electron micrographs and characterization. This material is available free of charge via the Internet at http://pubs.acs.org.

References

(1) (a) *The Chemistry and Physics of Carbon*; Radovic, L. R., Ed.; Marcel Dekker: New York, 2001; Vol. 27. (b) Rodriguez-Reinoso, F.; Sepulveda-Escribano, A. *Hand. Surf. Interfaces Mater.* **2001**, *5*, 309−355.

(2) Rodriguez-Reinoso, F. *Handb. Porous Solids* **2002**, *3*, 1766−1827.

(3) (a) Sankintuna, B.; Yürüm, Y. *Ind. Eng. Chem. Res.* **2005**, *44*, 2893−2902. (b) Lee, J.; Han, S.; Hyeon, T. *J. Mater. Chem.* **2004**, *14*, 478−486. (c) Ryoo, R.; Joo, S. H.; Kruk, M.; Jaroniec, M. *Adv. Mater.* **2001**, *13*, 677−681. (d) Joo, S. H.; Choi, S. J.; Oh, I.; Kwak, J.; Liu, Z.; Terasaki, O.; Ryoo, R. *Nature* **2001**, *412*, 169−172. (e) Foley, H. C. *J. Microporous Mater.* **1995**, *4*, 407−433.

(4) (a) Fricke, J.; Petricevic, R. *Handb. Porous Solids* **2002**, *3*, 2037−2062. (b) Pekala, R. W.; Alviso, C. T.; Lu, X. *J. Non-Cryst. Solids* **1995**, *188*, 34−40. (c) Kyotani, T. *Carbon* **2000**, *38*, 269−286.

(5) (a) Han, B.; Zhou, W.; Sayari, A. *J. Am. Chem. Soc.* **2003**, *125*, 3222−3445. (b) Liang, C.; Hong, K.; Guiochon, G. A.; Mays, J. W.; Dai, S. *Angew. Chem.* **2004**, *43*, 5785−5789. (c) Pang, J.; Li, X.; Wang, D.; Wu, Z.; John, V. T.; Yang, Z.; Lu, Y. *Adv. Mater.* **2004**, *16*, 884−886.

(6) (a) Skrabalak, S. E.; Suslick, K. S. *J. Am. Chem. Soc.* **2005**, *127*, 9990−9991. (b) Suh, W. H.; Suslick, K. S. *J. Am. Chem. Soc.* **2005**, *127*, 12007−12010. (c) Didenko, Y. T.; Suslick, K. S. *J. Am. Chem. Soc.* **2005**, *127*, 12196−12197. (d) Messing, G. L.; Zhang, S. C.; Jayanthi, G. V. *J. Am. Ceram. Soc.* **1993**, *76*, 2707−2726. (e) Patil, P. S. *Mater. Chem. Phys.* **1999**, *59*, 185−198.

(7) (a) Epple, M.; Tröger, L. *J. Chem. Soc., Dalton Trans.* **1996**, 11−16. (b) Hines, D.; Bagreev, A.; Bandosz, T. J. *Langmuir* **2004**, *20*, 3388−3397. (c) Kamegawa, K.; Kodama, M.; Nishikubo, K.; Yamada, H.; Adachi, Y.; Yoshida, H. *Microporous Mesoporous Mater.* **2005**, *87*, 118−123.

(8) Wiersum, U. E.; Jenneskens, L. W. *Gas Phase Reactions in Organic Synthesis*; Gordon & Breach: Amsterdam, The Netherlands, 1997; pp 143−194.

(9) Kodas, T. T.; Hampden-Smith, M. *Aerosol Processing of Materials*; Wiley-VCH: New York, 1999.

JA064899H